

# Specific abrogation of transforming growth factor- $\beta$ signaling in T cells alters atherosclerotic lesion size and composition in mice

Andrea Gojova, Valérie Brun, Bruno Esposito, Françoise Cottrez, Pierre Gourdy, Patrice Ardouin, Alain Tedgui, Ziad Mallat, and Hervé Groux

**A large body of evidence supports a role for proinflammatory mediators in atherosclerotic disease progression and instability. However, only few endogenous mechanisms have been suggested that could alter disease progression. One such mechanism is thought to be mediated by transforming growth factor  $\beta$  (TGF- $\beta$ ). Transgenic mice that express a dominant-negative TGF- $\beta$  receptor type II under a T-cell-specific promoter were generated. Bone marrow transplantation from transgenic mice into irradiated low density**

**lipoprotein receptor knock-out (LDLr KO) mice, subsequently fed an atherogenic diet, resulted in T-cell-specific blockade of TGF- $\beta$  signaling in the recipient mice and increased differentiation of T cells toward both T helper 1 (Th1) and Th2 phenotypes. These mice showed a significant decrease in atherosclerotic lesion size in the aortic sinus compared with mice receiving transplants with the wild-type bone marrow. Atherosclerotic plaques of mice receiving transplants with the transgenic bone marrow showed in-**

**creased T-cell infiltration and expression of major histocompatibility complex (MHC) class II, along with a decrease in smooth muscle cell and collagen content, a plaque phenotype that is potentially vulnerable to rupture. These results identify for the first time an important role for specific and selective T-cell-TGF- $\beta$  signaling in atherosclerosis. (Blood. 2003;102:4052-4058)**

© 2003 by The American Society of Hematology

## Introduction

Atherosclerosis is a disease of the arterial wall that carries high morbidity and mortality. An asymptomatic stable atherosclerotic plaque is characterized by a small lipid core, composed of modified lipids, macrophages, and T cells, which is separated from the lumen vessel by a thick fibrous cap, composed of vascular smooth muscle cells secreting a solid collagen matrix.<sup>1</sup> Severe clinical manifestations of atherosclerosis (sudden death, myocardial infarction, stroke) are due to atherosclerotic plaque disruption that favors the direct contact between the thrombogenic lipid core and the circulating blood, leading to occlusion of the lumen vessel.<sup>1,2</sup> These unstable plaques are characterized by increased accumulation of activated inflammatory cells (macrophages and T lymphocytes) that infiltrate the fibrous cap and induce substantial loss in both vascular smooth muscle cell and collagen, leading to fibrous cap destabilization and disruption.<sup>1,2</sup>

Although a large body of evidence supports a role for proinflammatory mediators in disease progression and instability,<sup>1,2</sup> only few endogenous mechanisms have been suggested that could halt disease progression and preserve plaque stability. Studies have shown that anti-inflammatory cytokines with deactivating properties on macrophages and/or T cells may be produced within the atherosclerotic lesion.<sup>3-5</sup> Among the anti-inflammatory cytokines, interleukin 10 (IL-10) has been consistently shown to play a critical protective role in experimental atherosclerosis.<sup>6-8</sup> In addition to IL-10, recent data suggested a protective role for transforming growth factor  $\beta$  (TGF- $\beta$ ) against the development of atherosclerotic plaques with inflammatory phenotype.<sup>9,10</sup> However, those

studies used systemic injection of either anti-TGF- $\beta$  antibody<sup>9</sup> or recombinant soluble TGF- $\beta$  type II receptor,<sup>10</sup> which resulted in wide-range inhibition of TGF- $\beta$  activity in many cell types and favored excess inflammatory changes in the heart and vessels when using anti-TGF- $\beta$  antibody.<sup>9</sup> To overcome these drawbacks and to examine the role of specific and T-cell-selective TGF- $\beta$  signaling in atherosclerosis, we developed transgenic mice that express a dominant-negative TGF- $\beta$  receptor type II under a T-cell-specific promoter (CD2-dnTGFBR2). These mice, whose T cells are insensitive to TGF- $\beta$  signaling, were used to perform bone marrow transplantation into irradiated low density lipoprotein receptor knock-out (LDLr KO) mice. Atherosclerotic plaque size and composition were compared between LDLr KO mice receiving transplants with either CD2-dnTGFBR2 transgenic or control bone marrow and fed a high-fat atherogenic diet.

## Materials and methods

### Generation of transgenic mice

The human TGF- $\beta$  type II receptor sequence between nucleotides  $-7$  and  $+573$ , which encodes the extracellular and transmembrane portions of the TGF- $\beta$  type II receptor,<sup>11</sup> was cloned and amplified by using primers with flanking *EcoRI* sites and cloned into the hCD2 minigen plasmid, a generous gift from Dr D. Kioussis (National Institute for Medical Research, London, United Kingdom).<sup>12</sup> The sequence of dnTGFBR2 was confirmed by sequencing. To generate transgenic mice (Tg<sup>+</sup>), the CD2-dnTGFBR2 fragment was excised of plasmid sequences by *KpnI*, *XbaI*, purified, and

From the Institut National de la Santé et de la Recherche Médicale (INSERM) U541, Institut Fédératif de Recherche "Circulation Paris VII," Hôpital Lariboisière, Paris, France; TxCell, Bâtiment. ARC and INSERM U343, Hôpital de l'Archet, Nice, France; INSERM U397, Toulouse, France; and Institut Gustave Roussy, Villejuif, France.

Z.M. and H.G. share senior authorship of this paper.

**Reprints:** Ziad Mallat, INSERM U541, Hôpital Lariboisière, 41 Bd de la chapelle, 75010 Paris, France; e-mail: mallat@larib.inserm.fr.

The publication costs of this article were defrayed in part by page charge payment. Therefore, and solely to indicate this fact, this article is hereby marked "advertisement" in accordance with 18 U.S.C. section 1734.

© 2003 by The American Society of Hematology

Submitted May 29, 2003; accepted August 3, 2003. Prepublished online as *Blood* First Edition Paper, August 14, 2003; DOI 10.1182/blood-2003-05-1729.

injected into (C57BL/6  $\times$  C3H)F1 fertilized eggs. Founder mice were identified by using polymerase chain reaction (PCR) and backcrossed for 7 generations onto C57BL/6 background for further experiments. Mice displayed a similar phenotype as the one described by Gorelik and Flavell<sup>13</sup> with mild to moderate inflammatory infiltrates in old mice and spontaneous differentiation of T cells to T helper 1 (Th1)/Th2 phenotype.

### Cytokine assays

Sandwich enzyme-linked immunosorbent assays (ELISAs) were used to measure IL-4, IL-5, IL-10, and interferon  $\gamma$  (IFN- $\gamma$ ) as previously described.<sup>14</sup> In brief, ELISA plates (VWR International, Fontenay-Sous-bois, France) were coated with the appropriate anticytokine antibodies (Abs; 11B11, TRFK4, 2A5, and XGM1.2 for IL-4, IL-5, IL-10, and IFN- $\gamma$ , respectively) and incubated at 4°C overnight. After incubation, plates were blocked for 30 minutes at room temperature by adding 150  $\mu$ L 20% fetal calf serum/phosphate-buffered saline (FCS/PBS) to each well. Supernatants from in vitro-stimulated purified splenocytes were diluted in 5% FCS Yssel medium and added at a volume of 50  $\mu$ L/well. Plates were incubated overnight at 4°C and washed, and then the second-step Ab (24G2, TRFK5, SXC1, and R4-6A2 for IL-4, IL-5, IL-10, and IFN- $\gamma$ , respectively) was added at 50  $\mu$ L/well. Plates were incubated for 1 hour at room temperature and washed, and then the enzyme conjugate was added to each well. Plates were incubated at room temperature for 1 hour, after which time they were washed, and substrate 100  $\mu$ L/well was added, containing 1 mg/mL 2,2'-azino-bis (3-ethylbenzthiazolinesulfoni acid) (Sigma, St Quentin-Fallavier, France), 0.0003% H<sub>2</sub>O<sub>2</sub> in Na<sub>2</sub>HPO<sub>4</sub>, and 0.05 M citric acid. After the substrate had developed, 50  $\mu$ L of 0.2 M citric acid solution was added to each well to stop the reaction. The plates were then read on an ELISA reader (Labsystems iEMS reader, Helsinki, Finland).

### PCR analysis

DNA isolated from splenocytes was purified by phenol/chloroform extraction. PCR analysis was performed with the following specific primers (Figure 1A): 5' CD2 promoter, TAAATTTGTAGCCAGCTTCTTCTG; 3' TGFBR, ACCGGTCAGTCAGGATTGCTGGTGTATATTC. PCR cycles were 1 minute at 94°C, 1 minute at 60°C, and 1 minute at 72°C for 40 cycles. The specific amplified product is 702-base pair (bp) long. PCR products were analyzed on agarose gels stained with ethidium bromide.

### Bone marrow transplantation

For bone marrow transplantation experiments, we used LDLr KO mice because these mice, unlike apolipoprotein E (apoE) KO mice, still develop hypercholesterolemia following repopulation with bone marrow cells expressing the corresponding lipoprotein receptor. Fifteen male C57BL/6 LDLr KO mice obtained from Dr F. Bayard (INSERM U397, Toulouse, France) and bred in-house (8 weeks old) were subjected to 9.5-Gy lethal total body irradiation to eliminate endogenous bone marrow stem cells and bone marrow-derived cells. Eight mice were reconstituted, intravenously as previously described,<sup>15</sup> with bone marrow cells ( $3 \times 10^6$ ) extracted from the femur and tibia of 2 CD2-dnTGFBRII transgenic male mice, whereas 7 mice were equally reconstituted with bone marrow cells from 2 control littermates (control group). Following irradiation and bone marrow transplantation, mice were allowed to recover for 4 weeks under a chow diet and were then switched to a high-fat atherogenic diet (15% fat, 1.25% cholesterol, no cholate) for an additional 10 weeks to induce atherosclerotic lesion formation. Mice were kept in accordance with standard animal care requirements, housed 3 to 4 per cage, and maintained on a 12-hour light-dark cycle. The mice were housed under conventional conditions.

### Cell purification and culture

CD4<sup>+</sup> or CD8<sup>+</sup> cells were purified from spleen by negative selection using anti-CD11b (M1/70), anti-B220, anti-NK (natural killer) cells (DX5), and anti-CD8 or anti-CD4 monoclonal antibodies (mAbs), respectively, followed by depletion with a mixture of magnetic beads coated with antirat immunoglobulin (Dyna, Oslo, Norway). The purity of cells was usually more than 90%. Antigen-presenting cells (APCs) were prepared from splenocytes after T-cell depletion by using anti-CD3 mAb (2C11) and magnetic beads and irradiated at 3000 rad.

Purified CD4<sup>+</sup> or CD8<sup>+</sup> from 6-week-old Tg<sup>+</sup> and control mice were stimulated with anti-CD3 mAb (5  $\mu$ g/mL) and anti-CD28 (10  $\mu$ g/mL) precoated on plastic wells in 96-well plates for 72 hours in the presence or absence of 3 ng/mL TGF- $\beta$ 1. Purified B cells (B220<sup>+</sup>) were stimulated with 10  $\mu$ g/mL lipopolysaccharide (LPS) for 48 hours with or without 3 ng/mL TGF- $\beta$ 1. One microcurie (37 KBq) per well of [<sup>3</sup>H]-thymidine (Perkin Elmer, Shelton, CT) was added for the last 8 hours of culture.

For the cell proliferation assay in irradiated mice reconstituted with bone marrow cells, purified T cells ( $2 \times 10^4$ ) were mixed with irradiated splenic APCs ( $4 \times 10^5$ ) and concanavalin A (con A; 0.5  $\mu$ g/mL; Sigma) with or without

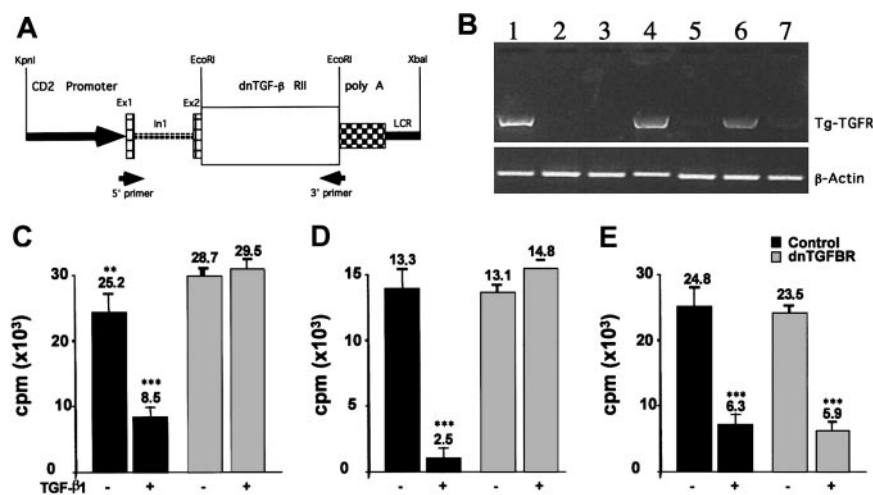


**Figure 1. Generation and characterization of CD2-dnTGFBRII transgenic mice.** (A) Schematic representation (not to scale) of CD2-dnTGFBRII construct. The open box represents extracellular and transmembrane portions of human TGF- $\beta$  receptor type II between nucleotides -7 and +573 followed by a stop codon. Primers used for PCR analysis of the transgene insertion in transgene-positive mice are also shown. (B) RT-PCR performed using primers indicated in panel A for the Tg-TGFR-specific transcript or with primers specific for  $\beta$ -actin as control on cDNA isolated from total splenocytes (lane 1), purified B cells (lane 2 and 1/10 lane 3), purified CD4<sup>+</sup> T cells (lane 4 and 1/10 lane 5), and purified CD8<sup>+</sup> T cells (lane 6 and 1/10 lane 7). (C-E) Purified CD4<sup>+</sup> (C) or CD8<sup>+</sup> (D) from 6-week-old Tg<sup>+</sup> and control mice were stimulated with anti-CD3 mAb (5  $\mu$ g/mL) and anti-CD28 (10  $\mu$ g/mL) precoated on plastic wells in 96-well plates for 72 hours in the presence or absence of 3 ng/mL TGF- $\beta$ 1. B220<sup>+</sup> cells (E) were stimulated with 10  $\mu$ g/mL LPS for 48 hours. One microcurie (0.037 MBq) per well of [<sup>3</sup>H]thymidine was added for the last 8 hours of culture. \*\* indicates statistically significant decrease ( $P < .01$ ;  $n = 4$ ) in [<sup>3</sup>H]thymidine incorporation between control and Tg<sup>+</sup> mice; \*\*\*, statistically significant decrease ( $P < .01$ ;  $n = 4$ ) in [<sup>3</sup>H]thymidine incorporation in the presence of exogenously added TGF- $\beta$ 1. Numbers above bars indicate mean values. Error bars show SEM.

TGF- $\beta$ 1 (1 ng/mL; R&D Systems, Abingdon, United Kingdom) in 200  $\mu$ L in 96-well plates. The cells were stimulated for 72 hours, and 1  $\mu$ C (37 KBq) [ $^3$ H]-thymidine (Perkin Elmer) was added for the last 10 hours of cell culture.

For cytokine production measurements, purified T cells ( $10^5$ ) were mixed with irradiated splenic APCs ( $4 \times 10^5$ ) and con A (5  $\mu$ g/mL; Sigma) in 96-well plates. Supernatants were collected at 24 hours (for IL-4 measurements) and at 48 hours (for IL-10, IL-5, and IFN- $\gamma$  measurements) and assayed for cytokine levels by ELISA.

### Analysis of atherosclerotic plaque size and composition

At 22 weeks of age, mice were anesthetized by isoflurane inhalation. Blood was drawn from the retroorbital venous plexus, and plasma cholesterol and high density lipoprotein (HDL) cholesterol were measured with a commercially available Cholesterol kit (Sigma). The anesthetized mice were killed by CO<sub>2</sub> overdose. The basal half of the ventricles and the ascending aorta were perfusion-fixed in situ with 4% paraformaldehyde. Then, they were removed, transferred to a PBS-30% sucrose solution, embedded in frozen optimal cutting temperature compound (OCT), and stored at  $-70^\circ\text{C}$ . Serial 8- to 10- $\mu$ m sections of the aortic sinus with valves (60-80 per mouse) were cut on a cryostat. Of every 5 sections, 1 section was kept for detection of lipid deposition with Oil red O staining. The other sections were dedicated to immunohistologic analysis and collagen detection.<sup>16</sup> Collagen fibers were stained with Sirius red. Morphometric analysis was performed with an automated image processor (Microvision; Histolab, Evry, France). The lesion collagen content was determined by measuring the relative area/density in 12 contiguous fields in each Sirius red-stained section.<sup>16</sup>

The thoracoabdominal aortas, spanning from the left subclavian artery to the renal arteries, were fixed with 4% paraformaldehyde and stained for lipid deposition with Oil red. They were then opened longitudinally, and the percentage of lipid deposition was calculated using computer-assisted image semiquantification (Microvision; Histolab).<sup>16</sup>

Immunohistochemical analysis was performed as previously described.<sup>16</sup> The following primary antibodies were used: MOMA-2 (monocyte macrophage marker 2), a rat antimouse monoclonal antibody (BioSource, Nivelles, Belgium) at a dilution 1:30 as a specific marker for macrophage; antimouse CD 3- $\epsilon$ , a goat polyclonal antibody (Santa Cruz, Santa Cruz, CA) at a dilution 1:100; anti- $\alpha$ -smooth muscle actin, clone 1A4, a mouse monoclonal antibody, alkaline phosphatase conjugate (Sigma) at a dilution of 1:50; antimouse MHC class II, a rat monoclonal antibody (BioSource) at a dilution of 1:10; antimouse goat polyclonal CD1 antibody (Santa Cruz) at a dilution of 1:20. Immunostains were visualized after incubation with the corresponding secondary biotinylated antibodies (Vector Laboratories, Burlingame, CA) and the use of an avidin-biotin horseradish peroxidase visualization system (Vectastain ABC kit; Vector Laboratories). Irrelevant isotype-matched immunoglobulins were used as negative controls. At least 4 sections per animal were analyzed for each immunostaining. Morphometric analysis was performed as described.<sup>16</sup>

### Statistical analysis

The effects of transplantation of transgenic CD2-dnTGFBR2 or control bone marrow cells on lesion area and plaque composition were compared using either a *t* test or the Mann-Whitney test. Data are expressed as mean  $\pm$  SE. A value of *P* < .05 was considered to be statistically significant.

## Results

### Generation of hCD2- $\Delta$ TGFR2 mice

To interrupt TGF- $\beta$  signaling in T cells we inserted the cDNA of a truncated TGF- $\beta$  type II receptor ( $\Delta$ TGFR2) that lacks the intracellular kinase domain into the human CD2 minilocus expression vector (Figure 1A). The hCD2 promoter/enhancer drives the copy number-dependent expression in T cells.<sup>12</sup> We obtained 4 founder animals that were fertile and gave rise to 4 transgenic lines with no differences in transgene expression or responsiveness to TGF- $\beta$ . Heterozygous animals of all 4

lines showed no macroscopic abnormalities before the age of 6 months. As previously reported,<sup>13</sup> examination of hematoxylin and eosin-stained sections of various organs and tissues, including the stomach, duodenum, pancreas, kidney, colon, and lung, revealed signs of mild chronic inflammation after the age of 4 months with mild infiltration of leukocytes (data not shown).

Tissue-specific transgene expression was assessed by reverse transcriptase (RT)-PCR analysis. Total RNA was isolated from the total splenocytes or purified B cells and CD4<sup>+</sup> and CD8<sup>+</sup> T-cell subpopulations. No transgene expression was observed in the B-cell fraction, and a similar level of expression was detectable in both CD4<sup>+</sup> and CD8<sup>+</sup> T cells (Figure 1B) as previously shown with the same plasmid construction and different transgenes.

Next, the ability of the truncated receptor to compete with the endogenous TGF- $\beta$  type II receptor was assessed (Figure 1C-E). TGF- $\beta$  was added at various concentrations to splenocyte cultures. After purification and stimulation of T cells with anti-CD3 and anti-CD28 mAbs, a marked TGF- $\beta$ -mediated inhibition of proliferation of wild-type CD4<sup>+</sup> and CD8<sup>+</sup> T cells was noted. In contrast, proliferation of CD4<sup>+</sup> and CD8<sup>+</sup> transgenic T cells could not be inhibited even at a concentration of 10 ng/mL TGF- $\beta$ .

### Engraftment of CD2-dnTGFBR2 or control bone marrow cells into irradiated recipient LDLr KO mice

Peripheral blood cells and splenocytes were analyzed at the time of death. Circulating blood variables, including hematocrit, leukocyte, monocyte, and lymphocyte counts did not differ between LDLr KO mice that received transplants with the CD2-dnTGFBR2 bone marrow cells and mice that received the control cells (data not shown). The CD2-dnTGFBR2 transgene (Figure 1A) could be clearly identified in DNA of splenocytes from the dnTGFBR2 transplant group, but it was totally absent in splenocytes from the control transplant group (Figure 2A). Purified spleen T cells from the dnTGFBR2 group showed a 62% increase in con A-induced proliferative response compared with T cells from the control group (*P* = .004) (Figure 2B). Con A-induced proliferation of control T cells was significantly blocked in the presence of TGF- $\beta$ 1 (*P* = .0002), whereas dnTGFBR2 T cells were totally insensitive to the inhibitory effect of TGF- $\beta$ 1 (*P* = .60) (Figure 2B).

### Effect of inhibition of T-cell TGF- $\beta$ signaling on atherosclerotic lesion size

At 22 weeks of age (10 weeks of high-fat diet), animal weights, total plasma cholesterol, and HDL cholesterol levels were not different between the 2 groups (Table 1). Morphometric analysis of lipid deposition in the thoracoabdominal aorta showed no differences in the percentage of total atherosclerotic plaque area between the 2 groups (Table 1). However, we found a significant 29% decrease in lesion size (*P* = .04) at the level of the aortic sinus in mice in the dnTGFBR2 transplant group compared with the control group (Table 1), suggesting that T-cell-specific TGF- $\beta$  signaling contributes to lesion development.

### Effect of inhibition of T-cell TGF- $\beta$ signaling on atherosclerotic lesion composition

Because atherosclerotic lesion composition may determine plaque vulnerability to rupture in mice<sup>17-20</sup> and humans,<sup>21,22</sup> we examined in more detail atherosclerotic plaque composition in both dnTGFBR2 and control groups. To exclude any confounding effect related to differences in plaque size between the 2 groups, only sections with advanced plaques of similar size were included in the analysis

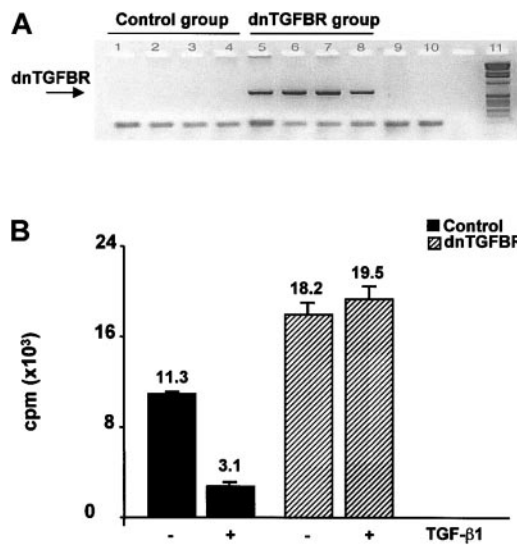


**Figure 2.** Characterization of irradiated LDLR KO mice transferred with either CD2-dnTGFBRII or control bone marrow. (A) PCR was performed using primers indicated in Figure 1 on DNA isolated from splenocytes of LDLR KO mice transferred with either a control bone marrow (1-4) or a CD2-dnTGFBRII bone marrow (5-8) to show the effective transfer and reconstitution of mice with the bone marrow of CD2-dnTGFBRII transgenic mice. Line 9 indicates no DNA; line 10, no PCR; line 11, molecular weight. (B) Proliferative response and TGF- $\beta$  function of splenocytes from control mice or mice reconstituted with CD2-dnTGFBRII transgenic bone marrow. Purified T cells isolated from spleens of control mice (■) or CD2-dnTGFBRII reconstituted mice (▨) were stimulated with both con A (0.5  $\mu$ g/mL) and irradiated T-depleted syngeneic normal splenocytes in the presence or absence of TGF- $\beta$ 1 (1 ng/mL) as indicated. Proliferation of triplicate culture was measured at day 3.  $P = .004$  between control and dnTGFBRII in the absence of TGF- $\beta$ 1;  $P = .0002$  between control with and control without TGF- $\beta$ 1. Numbers above bars indicate mean values. Error bars show SEM.

of plaque composition. Three to 4 sections per animal were studied. This analysis revealed important differences between the 2 groups of mice both in terms of cellular and matrix composition. Atherosclerotic lesions of the dnTGFBRII group showed a 68% increase in T-cell infiltration (CD3 staining) compared with the control mice ( $262 \pm 45$  cells/mm<sup>2</sup> of plaque area versus  $150 \pm 32$  cells/mm<sup>2</sup>, respectively,  $P = .04$ ) (Figure 3). The increase in inflammatory cell accumulation was restricted to T cells because we found no differences in the percentage of cross-sectional area occupied by macrophages (MOMA-2-positive staining) between the 2 groups ( $64.7\% \pm 2.3\%$  versus  $64.3\% \pm 3.1\%$ , respectively). However, we found a 2-fold increase in the accumulation of MHC class II-positive cells in plaques of mice from the dnTGFBRII group compared with the control group ( $89.8 \pm 16.9$  positive cells/mm<sup>2</sup> of plaque area versus  $44.6 \pm 12.7$  positive cells/mm<sup>2</sup>, respectively,  $P = .01$ ) (Figure 3). Although some CD1<sup>+</sup> dendritic cells showed positive MHC class II staining (Figure 4), these cells were only rarely detected within plaques and could not account for the marked accumulation of MHC class II-positive cells. In addition,

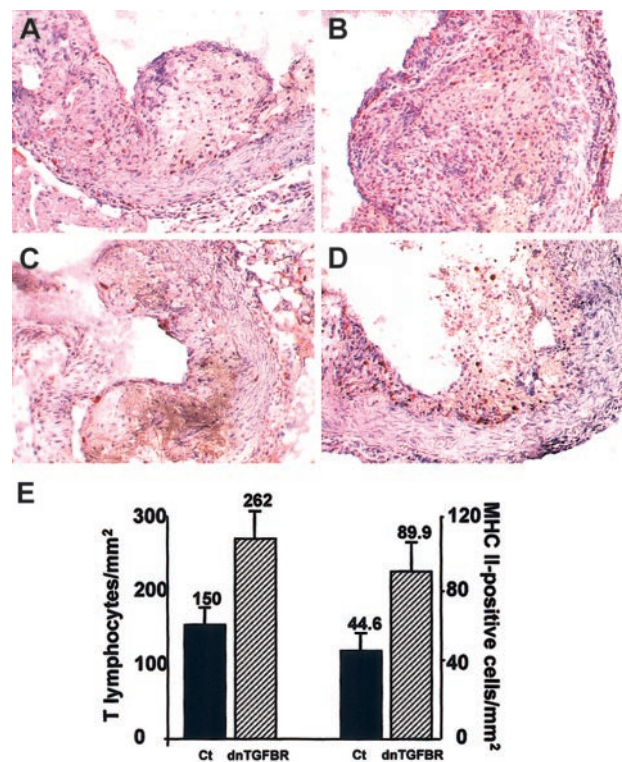


**Figure 3.** Inflammatory content of atherosclerotic lesions. Representative photomicrographs showing atherosclerotic lesions in the aortic sinus of control (A,C) or CD2-dnTGFBRII (B,D) LDLR KO mice. CD3 staining was detected by staining with antimouse CD 3- $\epsilon$  (small red spots in A and B). MHC class II expression in the lesions was detected by staining with antimouse MHC class II (small red spots in C and D). Original magnification,  $\times 200$ . (E) Quantitative analysis of CD3-positive (T lymphocytes) and MHC class II-positive cells in the atherosclerotic plaques of CD2-dnTGFBRII ( $n = 8$ ) and control (Ct;  $n = 7$ ) mice. Four to 5 sections per animal were analyzed for each immunostaining. Results are expressed as number of positive cells per mm<sup>2</sup> lesion area (numbers above bars  $\pm$  SEM).  $P < .05$  for T lymphocytes;  $P = .01$  for MHC class II.

no B cells (CD45R/B220) were detected within the plaques (data not shown), and only very few lipid core foam cells expressed MHC class II antigen (Figure 4). Most of the MHC class II-positive cells appeared to be macrophages located at the borders of the lipid core (Figure 4). Increased accumulation of MHC class II-positive cells and T cells was associated with significant loss of smooth muscle cells ( $\alpha$ -actin staining, Figure 5) in the plaques of dnTGFBRII transgenic mice compared with the plaques of control mice ( $7.7\% \pm 0.9\%$  versus  $11.6\% \pm 1.4\%$ , respectively,  $P = .03$ ). Moreover, quantitative analysis of collagen content (Sirius red staining, Figure 5) showed that collagen accumulation was significantly reduced in dnTGFBRII transgenic mice compared with the control mice ( $14.2\% \pm 0.9\%$  versus  $20.0\% \pm 2.0\%$ , respectively,  $P = .01$ ). Therefore, atherosclerotic plaques of dnTGFBRII transgenic mice showed increased accumulation of activated inflammatory cells

**Table 1. Weights, plasma total, and HDL cholesterol levels and atherosclerotic lesion size in control and CD2-dnTGFBRII groups**

	Control group, n = 7	CD2-dnTGFBRII group, n = 8
Weight, g	28.2 $\pm$ 1.2	26.9 $\pm$ 0.9
Total cholesterol, g/L (mM)	17.8 $\pm$ 1.5 (46.3 $\pm$ 3.9)	14.9 $\pm$ 0.7 (38.7 $\pm$ 1.8)
HDL cholesterol, g/L (mM)	0.7 $\pm$ 0.2 (1.8 $\pm$ 0.5)	0.8 $\pm$ 0.1 (2.1 $\pm$ 0.3)
Lesion size in thoracic aorta, %	9.3 $\pm$ 1.1	9.6 $\pm$ 1.5
Lesion size in aortic sinus, $\mu$ m <sup>2</sup>	212 341 $\pm$ 18 673	150 666 $\pm$ 19 055*

Data are means  $\pm$  SE.  
\* $P < .05$ .

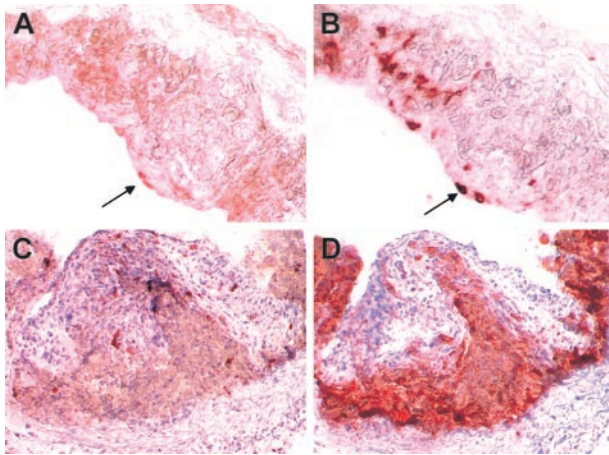


**Figure 4. Representative photomicrographs showing atherosclerotic lesions in the aortic sinus of CD2-dnTGFBR1I LDLr KO mice.** CD1 staining was detected using antimouse goat polyclonal CD1 antibody (arrow in panel A). Only few CD1<sup>+</sup> dendritic cells were detected. Although these cells expressed MHC class II (arrow in panel B), most of the MHC class II-positive cells stained negative for CD1 in an adjacent section (B). (C) MHC class II expression detected by staining with antimouse MHC class II. (D) Adjacent section stained with MOMA-2 to detect macrophages and foam cells. Most of the macrophages staining positively for MHC class II were disposed at the margins of the lipid core. Original magnification,  $\times 400$  (A-B); and  $\times 200$  (C-D).

along with a decrease in smooth muscle cell and collagen content, all factors that may contribute to the development of vulnerable plaques.

#### T-cell cytokine profile in CD2-dnTGFBR1I transgenic and control mice

To gain further insight into the mechanisms responsible for the differences in plaque size and composition in CD2-dnTGFBR1I transgenic mice, we analyzed con A–induced T-cell cytokine responses in cultured splenocytes from the 2 groups of irradiated and reconstituted mice. As shown in Figure 6, we found a significant increase in the production of IFN- $\gamma$  (Th1 and pro-atherogenic cytokine) and IL-4 and IL-5 (Th2 cytokines) by CD2-dnTGFBR1I transgenic T cells compared with those of the control group. Interestingly, production of IL-10, an antiatherogenic cytokine, was similar in the 2 groups of mice.

## Discussion

In the present study, we developed CD2-dnTGFBR1I transgenic mice whose T cells are totally insensitive to TGF- $\beta$  to examine the role of T-cell-specific abrogation of TGF- $\beta$  signaling in atherosclerosis. Bone marrow cells from these mice or from control mice were transplanted into irradiated LDLr KO mice that were subsequently fed a cholate-free high-fat atherogenic diet. The T-cell-specific inhibition of TGF- $\beta$  activity achieved in 1 of the 2 groups of mice receiving transplants had no effect on atherosclerotic lesion size in the thoracoabdominal aorta and resulted in a modest but significant decrease in lesion size in the aortic sinus, suggesting that endogenous T-cell-specific TGF- $\beta$  activity contributes to plaque burden, at least in some regions of the vascular tree.

Two previous studies have examined the role of specific but nonselective TGF- $\beta$  inhibition in apoE KO mice.<sup>9,10</sup> Lutgens et al<sup>10</sup> showed that inhibition of TGF- $\beta$  activity following systemic administration of a recombinant soluble TGF- $\beta$  type II receptor led to either no change or to a decrease in atherosclerotic lesion size,

depending on the time of treatment. In the other study, we observed an increase in atherosclerotic lesion size in the aortic sinus of mice housed under conventional conditions and treated with anti-TGF- $\beta$  antibody,<sup>9</sup> although a trend to reduced lesion size was observed when mice were housed in filtered cages (P.G., unpublished data, March 2002). Our present findings of reduced lesion size in the aortic sinus of mice with specific disruption of TGF- $\beta$  signaling in T cells highlights the importance of T-cell-specific TGF- $\beta$  activity in plaque development and the importance of dissecting the specific role of each cell type when investigating the role of TGF- $\beta$  in atherosclerosis.

The bulk of severe clinical manifestations of atherosclerosis has mainly been attributed to the disruption of small nonstenotic vulnerable or unstable plaques that are rich in inflammatory macrophages and T cells and are characterized by a thin fibrous cap with a substantial loss in extracellular matrix.<sup>21,22</sup> Recent studies in mice have also shown that ruptured plaques display many of the features of unstable plaques in humans.<sup>17,18</sup> Therefore, we examined the matrix and cell composition of arterial lesions in CD2-dnTGFBR1I and control groups. Lesions of CD2-dnTGFBR1I mice showed increased infiltration of T cells and increased expression of MHC class II without changes in the relative accumulation of

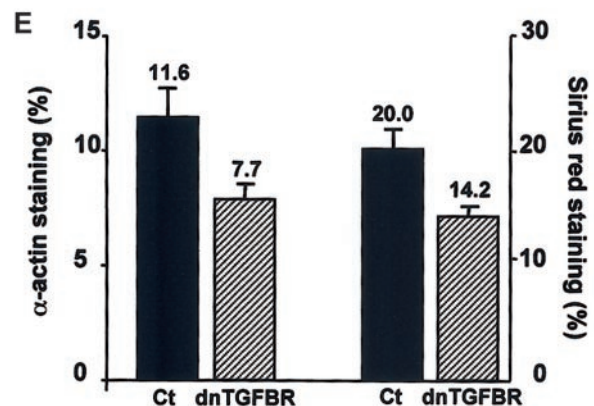
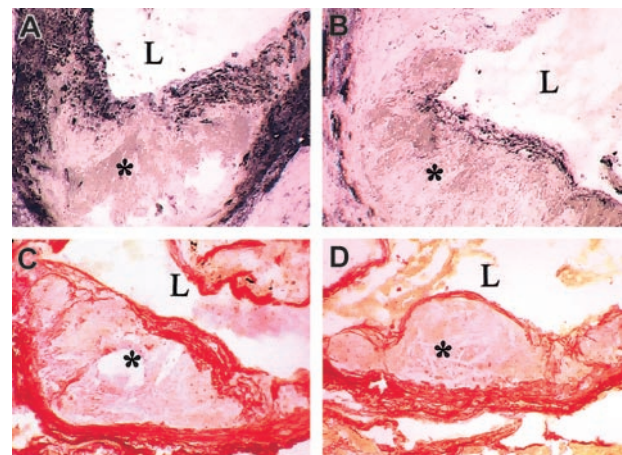
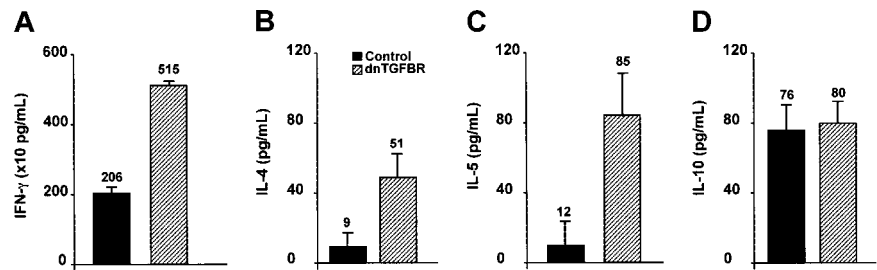


**Figure 5. Smooth muscle cell and collagen content of atherosclerotic lesions.** Representative photomicrographs showing atherosclerotic lesions in the aortic sinus of control (A,C) or CD2-dnTGFBR1I (B,D) LDLr KO mice. Smooth-muscle cell content was detected by staining with anti- $\alpha$ -actin antibody (black staining; A-B). Collagen content in the lesions was detected by staining with Sirius red (red staining; C-D). \* Indicates the intima; L, the lumen of the vessel. Original magnification,  $\times 400$ . (E) Quantitative analysis of  $\alpha$ -actin and Sirius red staining was performed using Histolab Microvision software. Four to 5 sections per animal were analyzed for each immunostaining;  $n = 7$  to 8 per group. Results (means  $\pm$  SE) are expressed as percentage of positive surface area.  $P = .03$  for actin and  $P = .01$  for Sirius red. Mean values are shown above bars.

**Figure 6. Cytokine profile of cultured spleen T cells from irradiated and reconstituted mice (n = 4 to 5 per group).** Th1 (IFN- $\gamma$ ) and Th2 (IL-4, IL-5, and IL-10) cytokine production in cultured spleen T cells 24 hours (for IL-4) or 48 hours (for IFN- $\gamma$ , IL-5, and IL-10) following stimulation with con A.  $P = .02$  for IFN- $\gamma$ , IL-4, and IL-5;  $P = .77$  for IL-10. We found a significant increase in IFN- $\gamma$  (A), IL-4 (B), and IL-5 (C) production in spleen T cells from dnTGFBR11 mice compared with controls. There was no difference in IL-10 production (D) between the 2 groups.



macrophages between the 2 groups. As expected, dendritic cells that were sparse within the lesions contributed to MHC class II expression. However, most of MHC class II positivity was associated with cells of monocytic/macrophage origin that have not matured into foam cells, although some expression by T cells or smooth muscle cells could not be excluded. The increased accumulation of activated MHC class II-positive cells and T cells in lesions of CD2-dnTGFBR11 mice was associated with a decrease in smooth muscle cell content and a lower percentage of collagen in comparison with lesions of control mice. These plaque features are compatible with the deactivating properties of TGF- $\beta$  on T cells<sup>13,23</sup> which could lead to increased IFN- $\gamma$  production (Figure 6) and increased MHC class II expression on monocytes/macrophages and are in agreement with the role of TGF- $\beta$  in matrix remodeling.<sup>24</sup> Our findings clearly show that specific inhibition of TGF- $\beta$  signaling in T cells leads to the development of atherosclerotic plaques with a phenotype that may potentially increase plaque vulnerability to rupture, strongly suggesting an important protective role of endogenous T-cell TGF- $\beta$  activity against vulnerability to atherosclerosis. Whether this effect of T-cell-specific TGF- $\beta$  signaling could also operate during more advanced stages of atherosclerosis and whether it could lead to plaque rupture remains to be determined. A potential limitation of this study is the absence of data on plaque composition in the thoracic aorta where lesion size was not affected. However, this is unlikely to significantly affect our interpretation because Lutgens et al<sup>10</sup> have reported changes in plaque composition indicative of larger lipid cores and thinner fibrous caps regardless of changes in plaque burden following specific but nonselective TGF- $\beta$  inhibition.

Immune mechanisms are involved in the atherosclerotic process,<sup>1,2,25</sup> and studies have unraveled a critical role for TGF- $\beta$  signaling in T-cell homeostasis.<sup>13,26,27</sup> In the present study, we found a significant increase in T-cell proliferative response to con A and a significant increase in both Th1- (IFN- $\gamma$ ) and Th2-specific (IL-4, IL-5) cytokine production in the dnTGFBR11 group compared with the control group. This hyperactivation of dnTGFBR11 transgenic T cells was associated with increased accumulation of

MHC class II-positive cells in the atherosclerotic lesions, indicating enhanced immune activation.<sup>28</sup> We hypothesize that these changes in T-cell responses, especially increased Th1 responses, may have contributed to the changes in plaque composition observed in the dnTGFBR11 group. It is unlikely that increased Th2 cytokine production could have played a major role in the differences in atherosclerotic plaque size and composition reported in the present study. IL-4 does not seem to affect lesion size or composition in the aortic root of LDLr KO mice,<sup>29</sup> and the production of IL-10 was similar in the 2 groups of mice. In contrast, the available evidence suggests that increased IFN- $\gamma$  production may have contributed to the alterations in cell and matrix composition reported in the dnTGFBR11 group of the present study. IFN- $\gamma$  inhibits smooth muscle cell proliferation<sup>30</sup> and collagen synthesis by smooth muscle cells<sup>31</sup> and may induce their apoptosis when associated with other proinflammatory cytokines.<sup>32</sup> Moreover, administration of IFN- $\gamma$  enhances plaque formation and inflammation,<sup>33</sup> and inhibition of IFN- $\gamma$  signaling leads to increased accumulation of collagen in plaques of apoE knock-out mice.<sup>16,34</sup> Nevertheless, further work is necessary to examine in more detail the specific contribution of Th1 and Th2 responses to the changes in plaque size and composition observed in the dnTGFBR11 group of the present study.

In conclusion, we show for the first time that specific abrogation of TGF- $\beta$  signaling in T cells is sufficient to induce the formation of atherosclerotic plaques with increased inflammatory cell component and decreased smooth muscle cell and collagen content, features that may increase the plaque vulnerability to rupture. These findings are associated with hyperactivation of spleen-derived T cells that produce high levels of both Th1- and Th2-specific cytokines other than IL-10.

## Acknowledgment

We thank Catherine Lacout (Institut Gustave Roussy, Villejuif, France) for her help in irradiation and transplantation experiments.

## References

- Lusis A. Atherosclerosis. *Nature*. 2000;407:233-241.
- Libby P. Current concepts of the pathogenesis of the acute coronary syndromes. *Circulation*. 2001;104:365-372.
- Uyemura K, Demer LL, Castle SC, et al. Cross-regulatory roles of interleukin (IL)-12 and IL-10 in atherosclerosis. *J Clin Invest*. 1996;97:2130-2138.
- Mallat Z, Heymes C, Ohan J, Faggin E, Lesèche G, Tedgui A. Expression of interleukin-10 in advanced human atherosclerotic plaques. Relation to inducible nitric oxide synthase expression and cell death. *Arterioscler Thromb Vasc Biol*. 1999;19:611-616.
- Bobik A, Agrotis A, Kanellakis P, et al. Distinct patterns of transforming growth factor- $\beta$  isoform and receptor expression in human atherosclerotic lesions. Colocalization implicates TGF- $\beta$  in fibro-fatty lesion development. *Circulation*. 1999;99:2883-2891.
- Pinderski OLJ, Hedrick CC, Olvera T, et al. Interleukin-10 blocks atherosclerotic events in vitro and in vivo. *Arterioscler Thromb Vasc Biol*. 1999;19:2847-2853.
- Mallat Z, Besnard S, Duriez M, et al. Protective role of interleukin-10 in atherosclerosis. *Circ Res*. 1999;85:e17-e24.
- Pinderski LJ, Fischbein MP, Subbanagounder G, et al. Overexpression of interleukin-10 by activated T lymphocytes inhibits atherosclerosis in LDL receptor-deficient mice by altering lymphocyte and macrophage phenotypes. *Circ Res*. 2002;90:1064-1071.
- Mallat Z, Gojova A, Marchiol-Fournigault C, et al. Inhibition of transforming growth factor-beta signaling accelerates atherosclerosis and induces an unstable plaque phenotype in mice. *Circ Res*. 2001;89:930-934.
- Lutgens E, Gijbels M, Smook M, et al. Transforming growth factor- $\beta$  mediates balance between inflammation and fibrosis during plaque progression. *Arterioscler Thromb Vasc Biol*. 2002;22:975-982.
- Bottlinger EP, Jakubczak JL, Roberts IS, et al. Expression of a dominant-negative mutant TGF-beta type II receptor in transgenic mice reveals essential roles for TGF-beta in regulation of

- growth and differentiation in the exocrine pancreas. *EMBO J*. 1997;16:2621-2633.
12. Zhumabekov T, Corbella P, Tolaini M, Kioussis D. Improved version of a human CD2 minigene based vector for T cell-specific expression in transgenic mice. *J Immunol Methods*. 1995;185:133-140.
  13. Gorelik L, Flavell RA. Abrogation of TGF $\beta$  signaling in T cells leads to spontaneous T cell differentiation and autoimmune disease. *Immunity*. 2000;12:171-181.
  14. Cottrez F, Hurst SD, Coffman RL, Groux H. T regulatory cells 1 inhibit a Th2-specific response in vivo. *J Immunol*. 2000;165:4848-4853.
  15. Boisvert WA, Spangenberg J, Kurtis LK. Treatment of severe hypercholesterolemia in apolipoprotein E-deficient mice by bone marrow transplantation. *J Clin Invest*. 1995;96:1118-1124.
  16. Mallat Z, Corbaz A, Scoazec A, et al. Interleukin-18/interleukin-18 binding protein signaling modulates atherosclerotic lesion development and stability. *Circ Res*. 2001;89:e41-e45.
  17. Williams H, Johnson JL, Carson KG, Jackson CL. Characteristics of intact and ruptured atherosclerotic plaques in brachiocephalic arteries of apolipoprotein E knockout mice. *Arterioscler Thromb Vasc Biol*. 2002;22:788-792.
  18. Bennett MR. Breaking the plaque: evidence for plaque rupture in animal models of atherosclerosis. *Arterioscler Thromb Vasc Biol*. 2002;22:713-714.
  19. Rosenfeld ME, Carson KG, Johnson JL, Williams H, Jackson CL, Schwartz SM. Animal models of spontaneous plaque rupture: the holy grail of experimental atherosclerosis research. *Curr Atheroscler Rep*. 2002;4:238-242.
  20. Calara F, Silvestre M, Casanada F, Yuan N, Napoli C, Palinski W. Spontaneous plaque rupture and secondary thrombosis in apolipoprotein E-deficient and LDL receptor-deficient mice. *J Pathol*. 2001;195:257-263.
  21. Virmani R, Kolodgie FD, Burke AP, Farb A, Schwartz SM. Lessons from sudden coronary death: a comprehensive morphological classification scheme for atherosclerotic lesions. *Arterioscler Thromb Vasc Biol*. 2000;20:1262-1275.
  22. Davies MJ. Stability and instability: two faces of coronary atherosclerosis—The Paul Dudley White Lecture 1995. *Circulation*. 1996;94:2013-2020.
  23. Topper JN. TGF- $\beta$  in the cardiovascular system: molecular mechanisms of a context-specific growth factor. *Trends Cardiovasc Med*. 2000;10:132-137.
  24. Border WA, Noble NA. Transforming growth factor- $\beta$  in tissue fibrosis. *N Engl J Med*. 1994;331:1286-1292.
  25. Hansson GK. Immune mechanisms in atherosclerosis. *Arterioscler Thromb Vasc Biol*. 2001;21:1876-1890.
  26. Lucas PJ, Kim SJ, Melby SJ, Gress RE. Disruption of T cell homeostasis in mice expressing a T cell-specific dominant negative transforming growth factor beta II receptor. *J Exp Med*. 2000;191:1187-1196.
  27. Nakao A, Miike S, Hatano M, et al. Blockade of transforming growth factor beta/Smad signaling in T cells by overexpression of Smad7 enhances antigen-induced airway inflammation and airway reactivity. *J Exp Med*. 2000;192:151-158.
  28. Jonasson L, Holm J, Skalli O, Gabbiani G, Hansson GK. Expression of class II transplantation antigen on vascular smooth muscle cells in human atherosclerosis. *J Clin Invest*. 1985;76:125-131.
  29. King VL, Szilvassy SJ, Daugherty A. Interleukin-4 deficiency decreases atherosclerotic lesion formation in a site-specific manner in female LDL receptor-/- mice. *Arterioscler Thromb Vasc Biol*. 2002;22:456-461.
  30. Hansson GK, Hellstrand M, Rymo L, Rubbia L, Gabbiani G. Interferon- $\gamma$  inhibits both proliferation and expression of differentiation-specific  $\alpha$ -smooth muscle actin in arterial smooth muscle cells. *J Exp Med*. 1989;170:1595-1608.
  31. Amento EP, Ehsani N, Palmer H, Libby P. Cytokines and growth factors positively and negatively regulate interstitial collagen gene expression in human vascular smooth muscle cells. *Arterioscler Thromb*. 1991;11:1223-1230.
  32. Geng YJ, Wu Q, Muszynski M, Hansson GK, Libby P. Apoptosis of vascular smooth muscle cells induced by in vitro stimulation with interferon-gamma, tumor necrosis factor-alpha, and interleukin-1 beta. *Arterioscler Thromb Vasc Biol*. 1996;16:19-27.
  33. Whitman SC, Ravisankar P, Elam H, Daugherty A. Exogenous interferon-gamma enhances atherosclerosis in apolipoprotein E-/- mice. *Am J Pathol*. 2000;157:1819-1824.
  34. Whitman SC, Ravisankar P, Daugherty A. Interleukin-18 enhances atherosclerosis in apolipoprotein E-/- mice through release of interferon- $\gamma$ . *Circ Res*. 2002;90:34e-38e.